Energy Loss Structure of X-ray Photoelectron Spectra of MgO and α-Al_2O_3

Shigemi Kohiki,*,†,‡ Masao Arai,‡ Hideki Yoshikawa,‡ and Sei Fukushima‡

Department of Materials Science, Kyusyu Institute of Technology, Tobata, Kita-kyusyu 804-8550, Japan, and National Institute for Research in Inorganic Materials, Tsukuba, Ibaraki 305-0044, Japan

Received: January 19, 1999; In Final Form: March 31, 1999

Experimental energy loss structures approximated by components at 11.3, 15.3, 18.3, and 23.2 eV for MgO and those at 14.5, 25.2, 35.3, and 49.9 eV for α-Al_2O_3 were compared with theoretical electron energy loss functions calculated from first principles using the full-potential linearized augmented plane wave method in the local density approximation. The electron energy loss functions, derived from the momentum matrix elements between Bloch functions, revealed that the experimental peaks at 23.2 eV for MgO and that at 25.2 eV for α-Al_2O_3 are due to bulk plasmon loss and the peak at 49.9 eV for α-Al_2O_3 is ascribed to the double losses of the plasmon excitation. The peaks at 11.3, 15.3, and 18.3 eV for MgO and those at 14.5 and 35.3 eV for α-Al_2O_3 result from the interband transitions from the valence band to the conduction band.

Introduction

X-ray photoelectron spectroscopy (XPS) is suitable to examine the electronic structure of the filled levels and dielectric response of a solid. During the approach of an excited electron to the solid surface, the Coulomb field accompanied with the moving electron interacts with the electrons of the solid via long-range dipole fields. The long-range Coulomb interactions bring about interband transitions and plasma excitations. High-resolution XPS can reveal the characteristic energy loss structure due to interband transition and plasmon excitation of the valence electrons on the lower kinetic energy side of core lines.

Electronic structures and dielectric functions of magnesium oxide (MgO) and sapphire (α-Al_2O_3) are of fundamental interest since the single crystals of MgO and α-Al_2O_3 are used widely as substrates for depositing thin films in basic science studies and microelectronic applications. Because the films are fabricated on the surfaces of the substrates, the properties of the thin films are inevitably affected by those of the substrates. The crystal structure of MgO is *Fm*3*m* [$a = 4.216$ Å][1] at room temperature (RT). The crystal structure of α-Al_2O_3 is *R*3*c* [$a = 5.13$ Å, $\alpha = 55.267°$], and the lattice constants of the corresponding hexagonal unit cell are $a = 4.76$ Å and $c = 13.00$ Å.[2] A number of experimental and theoretical studies of the electronic structure have been published for MgO[3−10] and α-Al_2O_3.[3,4,7,8,10−13]

For MgO, electronic interband transitions from about 8 to 20 eV have been reported with optical reflectance measurement[14] and explained theoretically.[5,6] Reported bulk plasmon energies by reflection electron energy loss measurement[14] and by the transmission electron energy loss measurement[15] were 22.0 and 23.2 eV, respectively. For α-Al_2O_3, interband transitions from a valence band to a conduction band and from the O 2s to a conduction band were observed at 13 and 32 eV by optical conductivity, respectively.[11] Previously reported electron energy loss functions were predicted only by the experimental optical energy loss function. In this paper, we elucidate the experimental photoelectron energy loss functions of MgO and α-Al_2O_3 using a first-principles computation of dielectric functions.

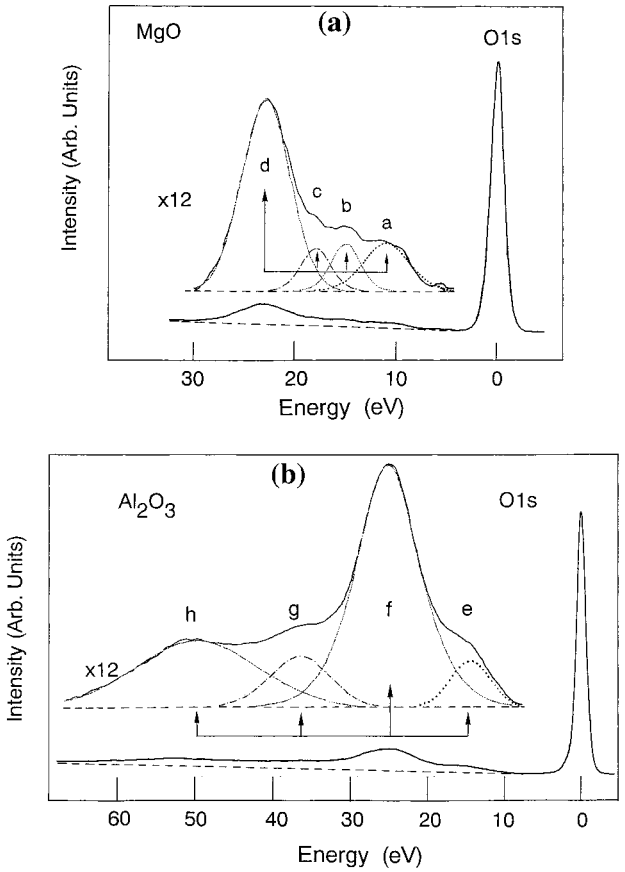

Figure 1. Experimental electron energy loss spectra of (a) MgO and (b) α-Al_2O_3.

Experimental Section

The spectra of a photoelectron excited with monochromatized Al Kα radiation were measured using a hemispherical electron

* Corresponding author. E-mail: kohiki@che.kyutech.ac.jp. Fax: +81-93-884-3300.
† Kyusyu Institute of Technology.
‡ National Institute for Research in Inorganic Materials.

10.1021/jp9901996 CCC: $18.00
Published on Web 06/06/1999

TABLE 1: Energy Loss Structure in MgO and α-Al_2O_3[a]

peak	separation (eV)	FWHM (eV)	intensity ratio	possible assignment
		MgO		
a	11.3	5.4	0.053	VB → CB
b	15.3	3.6	0.036	VB → CB
c	18.3	3.6	0.032	VB → CB
d	23.2	5.7	0.222	bulk plasmon
		α-Al_2O_3		
e	14.5	6.0	0.048	VB → CB
f	25.2	10.2	0.516	bulk plasmon
g	36.3	8.9	0.096	VB → CB
h	49.9	18.7	0.240	double losses of plasmon

[a] The values of separation and line intensity are relative to the zero loss line.

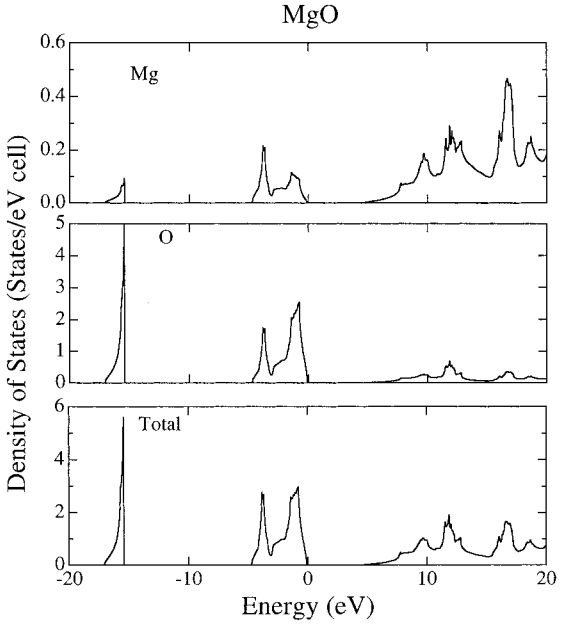

Figure 2. Calculated density of states (DOS) for MgO. Given as all of Mg and O and total DOS.

spectrometer under a pressure less than 5×10^{-8} Pa at RT. The spectrometer was calibrated utilizing Au $4f_{7/2}$ (83.9 eV) and Ag $3d_{5/2}$ (368.3 eV) electrons. The resolution of the spectrometer, defined as the full width at half-maximum (fwhm) of the Ag $3d_{5/2}$ was 0.59 eV. Single crystals of (100) orientation MgO with 0.5 mm thickness and (0001) orientation α-Al_2O_3 with 0.5 mm thickness were obtained from Tateho Chemical Co. and Kyocera Co., respectively. The samples were repeatedly cleaned in acetone and methanol with ultrasonic vibration and then transferred into the preparation chamber of the spectrometer. The samples showed a very small C 1s signals of the adventitious carbon (C−C and C−H) of the order of a submonolayer. As MgO and α-Al_2O_3 are insulators, charging effects were observed during X-ray irradiation. To stabilize the XPS spectra, the sample surface was flooded with low-energy (5 eV) electrons from a neutralizer, and the Fermi energy of the sample was determined from the C 1s electron binding energy (285.0 eV) of the adventitious carbon.

Results and Discussion

Core lines (O 1s, Mg 2p, Mg 2s, Al 2p, and Al 2s) are followed by an energy loss structure ranging from 5 to 30 eV for MgO and from 10 to 60 eV for α-Al_2O_3 relative to the zero loss line. Within the experimental uncertainty, the energy loss

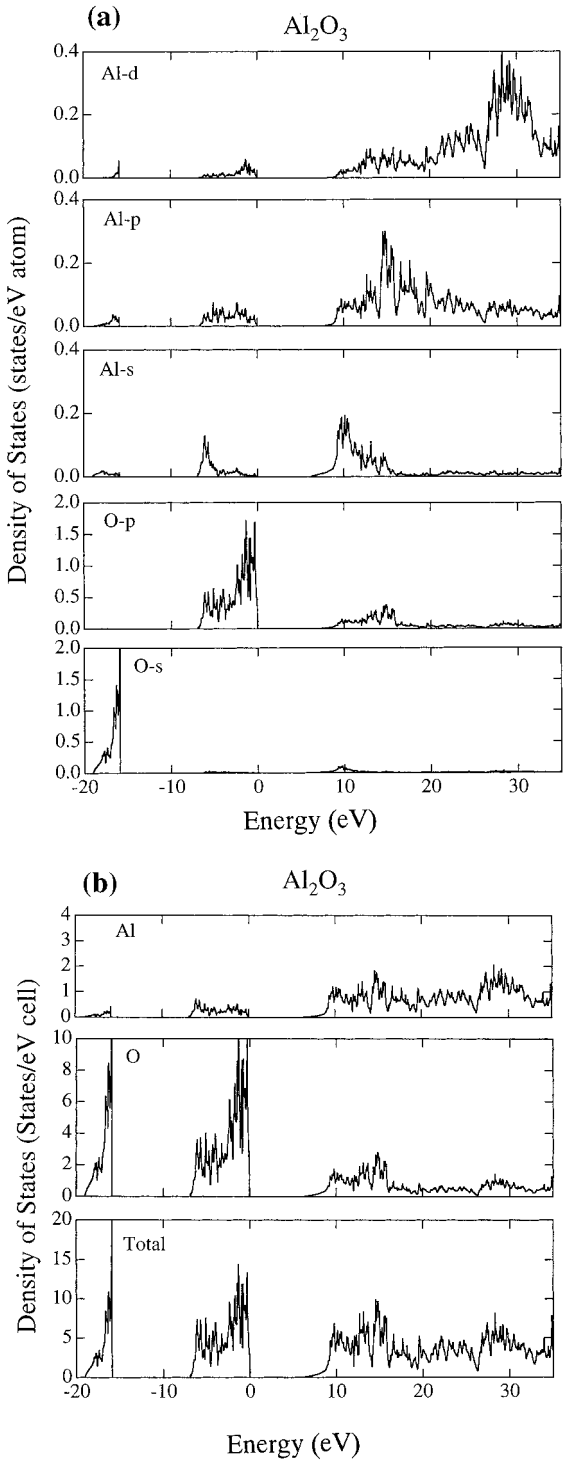

Figure 3. Calculated density of states (DOS) for α-Al_2O_3. Given as (a) partial DOS of Al 3d, 3p, 3s and O 2p, 2s orbitals and (b) all of Al and O and total DOS.

structure was the same for the lines with each material. The most intense and best resolved line is the O 1s for both MgO and α-Al_2O_3. The energy loss structures of the O 1s spectra of MgO and α-Al_2O_3 were different from each other. The energy loss spectra observed in this XPS are quite similar to those reported for MgO[4] and α-Al_2O_3.[7] As shown in parts a and b of Figure 1, the energy loss structures can be approximated by a sum of four components positioned at 11.3 (a), 15.3 (b), 18.3 (c), and 23.2 eV (d) for MgO and those positioned at 14.5 (e), 25.2 (f), 35.3 (g), and 49.9 eV (h) for α-Al_2O_3. The parameters of the energy loss peaks (a−h) are listed in Table 1.

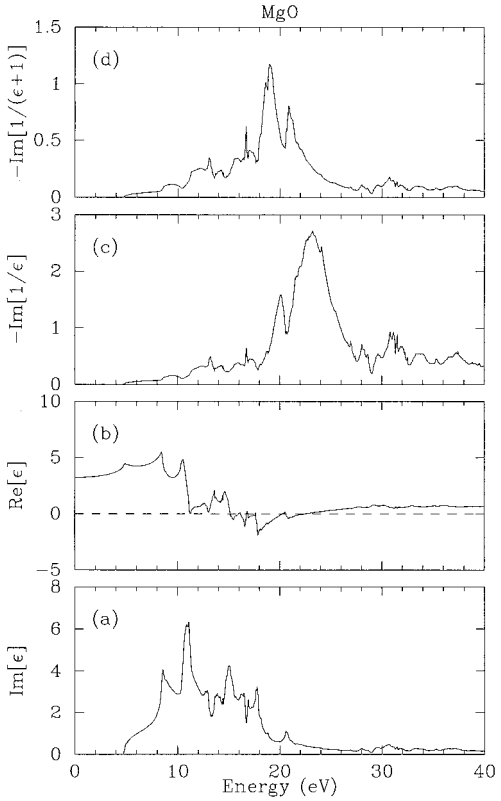

Figure 4. Calculated dielectric function and electron energy loss functions of MgO: (a) imaginary part and (b) real part of the theoretical dielectric function; (c) bulk and (d) surface electron energy loss functions.

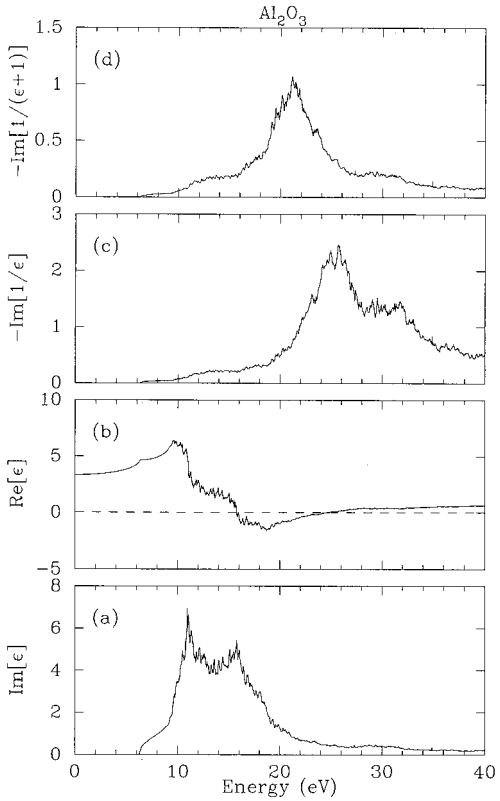

Figure 5. Calculated dielectric function and electron energy loss functions of α-Al_2O_3: (a) imaginary part and (b) real part of the theoretical dielectric function; (c) bulk and (d) surface electron energy loss functions.

We calculated the bulk electronic structures of MgO and α-Al_2O_3 within the local density approximation (LDA),[16] using the WIEN97 packages.[17] The LDA succeeded to describe the valence and conduction bands of various compounds.[16] However, the LDA fails to reproduce the band gaps of semiconductors and insulators. Typically, the band gap obtained by the LDA is only half of the experimental value. Thus, the transition energies between valence and conduction bands are also underestimated.

The calculated densities of states (DOS) of MgO and α-Al_2O_3 are shown in Figures 2 and 3, respectively. They are in good agreement with previous calculations.[6,8] The upper valence bands are mainly composed of the O 2p states which slightly hybridize with the metal s, p states. The lower valence bands below −15 eV are the O 2s bands.

The energy loss structures are generated by the inelastic scattering of photoexcited electrons. Within the Born approximation, the cross section of the inelastic scattering is related to dielectric functions ϵ as[18]

$$K(E_0,\omega) = \{-\mathrm{Im}[\epsilon(\omega)^{-1}]/\pi a_0 E_0\}\ \mathrm{In}\{[\sqrt{E_0} + \sqrt{(E_0-\hbar\omega)}\,]/[\sqrt{E_0} - \sqrt{(E_0-\hbar\omega)}]\}$$

where E_0 is the kinetic energy of electron and a_0 is the Bohr radius. Here the $\mathrm{Im}(\epsilon)^{-1}$ is assumed to be independent of the wave vector. Thus, the electron energy loss structures can be approximated by the $-\mathrm{Im}(\epsilon)^{-1}$ if we ignore multiple scattering effects.

The $\mathrm{Im}(\epsilon)$ was calculated from the momentum matrix elements between the occupied and unoccupied wave functions. The real part Re (ϵ) was evaluated from the $\mathrm{Im}(\epsilon)$ by the Kramers−Kronig transformation, and the $-\mathrm{Im}(\epsilon)^{-1}$ was obtained from the $\mathrm{Im}(\epsilon)$ and $\mathrm{Re}(\epsilon)$. We also calculated the $-\mathrm{Im}(\epsilon+1)^{-1}$ which is an approximation of the surface energy loss function since in XPS Ley et al.[19] has resolved surface plasmon peak clearly from bulk plasmon peak and the loss energies by XPS were in agreement with those by electron energy loss spectroscopy (EELS).[20]

The dielectric functions and energy loss functions of MgO and α-Al_2O_3 are shown in Figures 4 and 5, respectively. The broad structures at 10−20 eV in the $\mathrm{Im}(\epsilon)$ are due to the transition from the O 2p valence bands to the conduction bands. Above 20 eV, the $\mathrm{Im}(\epsilon)$ rapidly decreases and the plasmon peaks are clearly identified in the $-\mathrm{Im}(\epsilon)^{-1}$ at 23 eV for MgO and 26 eV for α-Al_2O_3. These energies are larger than the values estimated from the valence electron density, which are 21.0 eV for MgO and 24.0 eV for α-Al_2O_3. This indicates that the band structures influence the plasmon energies. In the surface energy loss function $-\mathrm{Im}(\epsilon+1)^{-1}$, the plasmon energies shift to the lower energy side by 4 eV for MgO and 5 eV for α-Al_2O_3.

There are small structures at around 30 eV in the $\mathrm{Im}(\epsilon)$ and $-\mathrm{Im}(\epsilon)^{-1}$. They arise from the broad peaks in the conduction bands at around 30 eV which is originated from the empty metal 3d states as shown in the DOS in Figures 2 and 3. The transitions from the O 2s bands to the conduction bands also appear at the same energy region.

From the calculated electron energy loss functions, the large experimental peaks at 23.2 eV for MgO and 25.2 eV for α-Al_2O_3 are assigned to the bulk plasmon loss. At higher energy, the experimental spectra of α-Al_2O_3 have two peaks. The highest peak at 49.9 eV for α-Al_2O_3 can be ascribed to the double losses of the plasmon excitation since the energy is twice as large as the plasmon energy. The peak at 35.3 eV for α-Al_2O_3 corresponds to the broad structure at around 30 eV in the calculated $-\mathrm{Im}(\epsilon)^{-1}$ and is caused by the empty Al 3d states. Below the

plasmon energies, the experimental spectra have several peaks for both MgO and α-Al_2O_3. These peaks correspond to the interband transition between O 2p valence bands and conduction bands.

Summary

We have presented the experimental and theoretical results on the photoelectron energy loss functions of MgO and α-Al_2O_3. A first-principles calculation can predict the energy loss structure in the core-level spectra of these compounds. As listed in Table 1, the energy loss structures at 11.3 (a), 15.3 (b), and 18.3 eV (c) for MgO were due to the interband transitions from the valence (filled O 2p) band to the conduction (empty Mg 3s and 3p) band, and that at 23.2 eV (d) was due to the bulk plasmon excitation. For α-Al_2O_3, the structures at 14.5 (e) and 35.3 eV (g) were due to the interband transitions from the valence (filled O 2p) band to the conduction (empty Al 3s and 3p) and (empty Al 3d) band, respectively. Those at 25.2 (f) and 49.9 eV (h) were due to a loss and double losses of bulk plasmon.

Acknowledgment. The authors thank T. Maruyama for assistance in the XPS measurement and P. Blaha, K. Schwarz, and J. Luiz for providing us their WIEN97 programs.

References and Notes

(1) Hirata, K.; Moriya, K.; Waseda, Y. *J. Mater. Sci.* **1977**, *12*, 838.

(2) Wyckoff, R. W. G. *Crystal Structures II*, 2nd ed.; Wiley: New York, 1964.

(3) Kohiki, S.; Fukushima, S.; Yoshikawa, H.; Arai, M. *Jpn. J. Appl. Phys.* **1997**, *36*, 2856; **1998**, *37*, 2078.

(4) Kowalczyk, S. P.; McFeely, F. R.; Ley, L.; Gritsyna, V. T.; Shirley, D. A. *Solid State Commun.* **1977**, *23*, 161 and references therein.

(5) Daude, N.; Jouanin, C.; Gout, C. *Phys. Rev. B* **1977**, *15*, 2399.

(6) Kotani, T. *Phys. Rev. B* **1994**, *50*, 14816.

(7) Gignac, W. J.; Williams, R. S.; Kowalczyk, S. P. *Phys. Rev. B* **1985**, *32*, 1237 and references therein.

(8) Xu, Yong-Nian; Ching, W. Y. *Phys. Rev. B* **1991**, *43*, 4461.

(9) Gibson. A.; Haydock, R.; LaFemina, J. P. *Phys. Rev. B* **1993**, *47*, 9229.

(10) O'Brien, W. L.; Jia, J.; Dong, Q.−Y.; Callcott, T. A.; Rubensson, J−E.; Mueller, D. L.; Ederer, D. L. *Phys. Rev. B* **1991**, *44*, 1013.

(11) French, R. H. *J. Am. Ceram. Soc.* **1990**, *73*, 477.

(12) Guo, J.; Ellis, D. E.; Lam, D. J. *Phys. Rev. B* **1992**, *45*, 3204.

(13) Guo, J.; Ellis, D. E.; Lam, D. J. *Phys. Rev. B* **1992**, *45*, 13647 and references therein.

(14) Roessler, D. M.; Walke, W. C. *Phys. Rev.* **1967**, *159*, 733.

(15) Venghaus, H. *Opt. Commun.* **1971**, *2*, 447.

(16) For a review, see: Jones, R. O.; Gunnarsson, O. *Rev. Mod. Phys.* **1989**, *61*, 689.

(17) Blaha, P.; Schwarz, K.; Luitz, J. *WIEN97*; Vienna University of Technology: Vienna, 1997. (Improved and updated UNIX version of the original copyrighted WIEN code, which was published in the following: Baha, P.; Schwarz, K.; Sorantin, P.; Tricky, S. B. *Comput. Phys. Commun.* **1990**, *59*, 399.)

(18) Mayer, B.; Mahl, S.; Neumann, M. Z. *Phys. B* **1996**, *101*, 85.

(19) Ley. L.; McFeely, F. R.; Kowalczyk, S. P.; Jenkin, S. P.; Shirley, D. A. *Phys. Rev. B* **1975**, *11*, 600.

(20) Powell, C. J.; Swan, J. B. *Phys. Rev. B* **1959**, *116*, 81.